Communication

Turning a Scorpion Toxin into an Antitumor Miniprotein

Chong Li, Min Liu, Juahdi Monbo, Guozhang Zou, Changqing Li, Weirong Yuan, Davide Zella, Wei-Yue Lu, and Wuyuan Lu

J. Am. Chem. Soc., **2008**, 130 (41), 13546-13548 • DOI: 10.1021/ja8042036 • Publication Date (Web): 18 September 2008

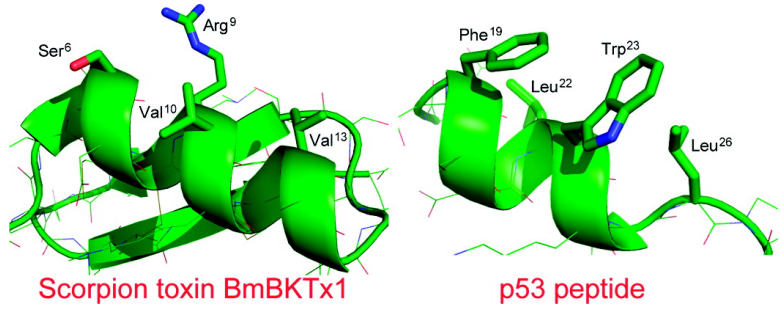

More About This Article

Additional resources and features associated with this article are available within the HTML version:

- Supporting Information
- Access to high resolution figures
- Links to articles and content related to this article
- Copyright permission to reproduce figures and/or text from this article

View the Full Text HTML

J|A|C|S
COMMUNICATIONS

Published on Web 09/18/2008

Turning a Scorpion Toxin into an Antitumor Miniprotein

Chong Li,[†,‡] Min Liu,[†] Juahdi Monbo,[†] Guozhang Zou,[†] Changqing Li,[†] Weirong Yuan,[†] Davide Zella,[†] Wei-Yue Lu,[‡] and Wuyuan Lu*[,†]

Institute of Human Virology, University of Maryland School of Medicine, 725 West Lombard Street, Baltimore, Maryland 21201, and School of Pharmacy, Fudan University, Shanghai 200032, China

Received June 4, 2008; E-mail: wlu@ihv.umaryland.edu

The oncoproteins MDM2 and MDMX negatively regulate the activity and stability of the tumor suppressor protein p53, a cellular process initiated by the binding of the N-terminal domain of MDM2 or MDMX to the transactivation domain of p53.[1] Gene amplification and overexpression of MDM2 and MDMX in many tumors confer p53 inactivation and tumor survival, making the two oncoproteins important molecular targets for anticancer therapy. Different classes of compounds have been designed to inhibit the p53-MDM2/MDMX interactions, many of which show efficacy in tumor killing by reactivating the p53 pathway *in vitro* and/or *in vivo*.[2] Among them are two miniature proteins, thioredoxin and pancreatic polypeptide that display the sequence of a peptide antagonist of MDM2/MDMX.[3] Here we report the design of a 27-residue miniprotein, termed stoppin (**s**corpion **to**xin-derived **p**otent **p**53-MDM2/MDMX **in**hibitor), derived from the K^+ channel blocker BmBKTx1 of the Asian scorpion *Buthus martensi* Karsch.[4] Stoppin competitively inhibits the p53-MDM2/MDMX interactions and efficiently kills tumor cells likely in a p53-dependent manner.

The N-terminal transactivation domain of p53 encompasses the sequence $T^{18}\mathbf{F}^{19}S^{20}D^{21}L^{22}\mathbf{W}^{23}K^{24}L^{25}\mathbf{L}^{26}$ minimally required for effective MDM2/MDMX binding.[5] Upon binding to the N-terminal domain of MDM2 or MDMX, $^{(18-26)}$p53 acquires a 2.5-turn α-helical structure, where the side chains of Phe^{19}, Trp^{23}, and Leu^{26} from p53 dock inside a hydrophobic cavity of the oncoproteins.[5] We previously synthesized the 31-amino acid residue BmBKTx1 (Scheme 1) whose structure was determined by both NMR spectroscopy and X-ray crystallography.[6] BmBKTx1 adopts a structural fold highly conserved in all short-chain K^+ channel toxins isolated from scorpion venom, a 3-turn N-terminal α-helix connected via three disulfide bonds to a C-terminal antiparallel β-sheet. Shown in Figure 1A are the N-terminal α-helix of BmBKTx1 and the helical segment of $^{(15-29)}$p53 seen in the complex with $^{(17-125)}$MDM2.[5] We replaced Ser^6, Arg^9, Val^{10}, and Val^{13} in BmBKTx1 with the topologically equivalent residues from p53 - Phe^{19}, Leu^{22}, Trp^{23}, and Leu^{26}. In addition, we deleted four terminal residues in BmBKTx1, Ala^1, Ala^2, Tyr^{30}, and Lys^{31}, resulting in a 27-residue peptide termed stoppin-1 of the following amino acid sequence: CYS**F**DC**L**W**K**C**L**AMGFSSGKCINSKCKC. Synthesis and oxidative folding of stoppin-1 is described in the Supporting Information (Figure S1).

Stoppin-1 adopts a partially α-helical conformation in aqueous solution, as indicated by its CD spectrum showing double minima at 208 and 222 nm and a positive peak at 195 nm (Figure S2, Supporting Information), consistent with the known structural features of BmBKTx1. One of the hallmarks of p53 interactions with MDM2/MDMX is the blue shift of Trp fluorescence, resulting from the burial of Trp^{23} into the hydrophobic cavity of MDM2/MDMX (unpublished results). Addition of a chemically synthesized p53-binding domain of MDM2 ($^{(25-109)}$MDM2, referred to thereafter as ^{syn}MDM2) to stoppin-1 caused a dramatic shift of Trp fluorescence by 28 nm (from 356 to 328 nm) (Figure 1B), suggesting that stoppin-1 binds to MDM2 in a way similar to p53 peptides. Similar results were obtained with stoppin-1 and ^{syn}MDMX ($^{(24-108)}$MDMX). We established a surface plasmon resonance (SPR) based method to quantify the binding affinity of stoppin-1 for ^{syn}MDM2 and ^{syn}MDMX, in which $^{(15-29)}$p53 was immobilized on a CM5 sensor chip for kinectic analysis of a fixed concentration of ^{syn}MDM2 (50 nM) or ^{syn}MDMX (100 nM) preincubated with varying concentrations of stoppin-1. $^{(15-29)}$p53 was used as a positive control in the competition binding assay. As shown in Figure 1C, stoppin-1 bound to ^{syn}MDM2 with a K_d value of 790 nM, while $^{(15-29)}$p53 bound to the same protein at an affinity of 123 nM. For ^{syn}MDMX, the K_d values of stoppin-1 and $^{(15-29)}$p53 were 994 and 279 nM, respectively. By contrast, BmBKTx1 did not bind either ^{syn}MDM2 or ^{syn}MDMX. Taken together, these results demonstrate the interaction between stoppin-1 and ^{syn}MDM2/^{syn}MDMX, validating the residue grafting approach to turning BmBKTx1 into a competitive inhibitor of the p53-MDM2/MDMX interactions.

Neither BmBKTx1 nor stoppin-1 was active in tumor killing assays (data not shown). The inability of stoppin-1 to kill tumor cells is attributable presumably to its failure to traverse the cell membrane. Cationic peptides are capable of promoting efficient cellular uptake of covalently attached proteins and peptides to the cytoplasm and nucleus of many cells through endocytosis.[7] To facilitate stoppin uptake by tumor cells, we re-engineered stoppin-1 by making five additional substitutions in its C-terminal region, resulting in a heavily cationic new peptide termed stoppin-2. Specifically, we replaced Ser^{18}, Ser^{19}, Ile^{23}, Asn^{24}, and Ser^{25}

Scheme 1. Amino Acid Sequence of BmBKTx1

[†] University of Maryland School of Medicine.
[‡] Fudan University.

10.1021/ja8042036 CCC: $40.75

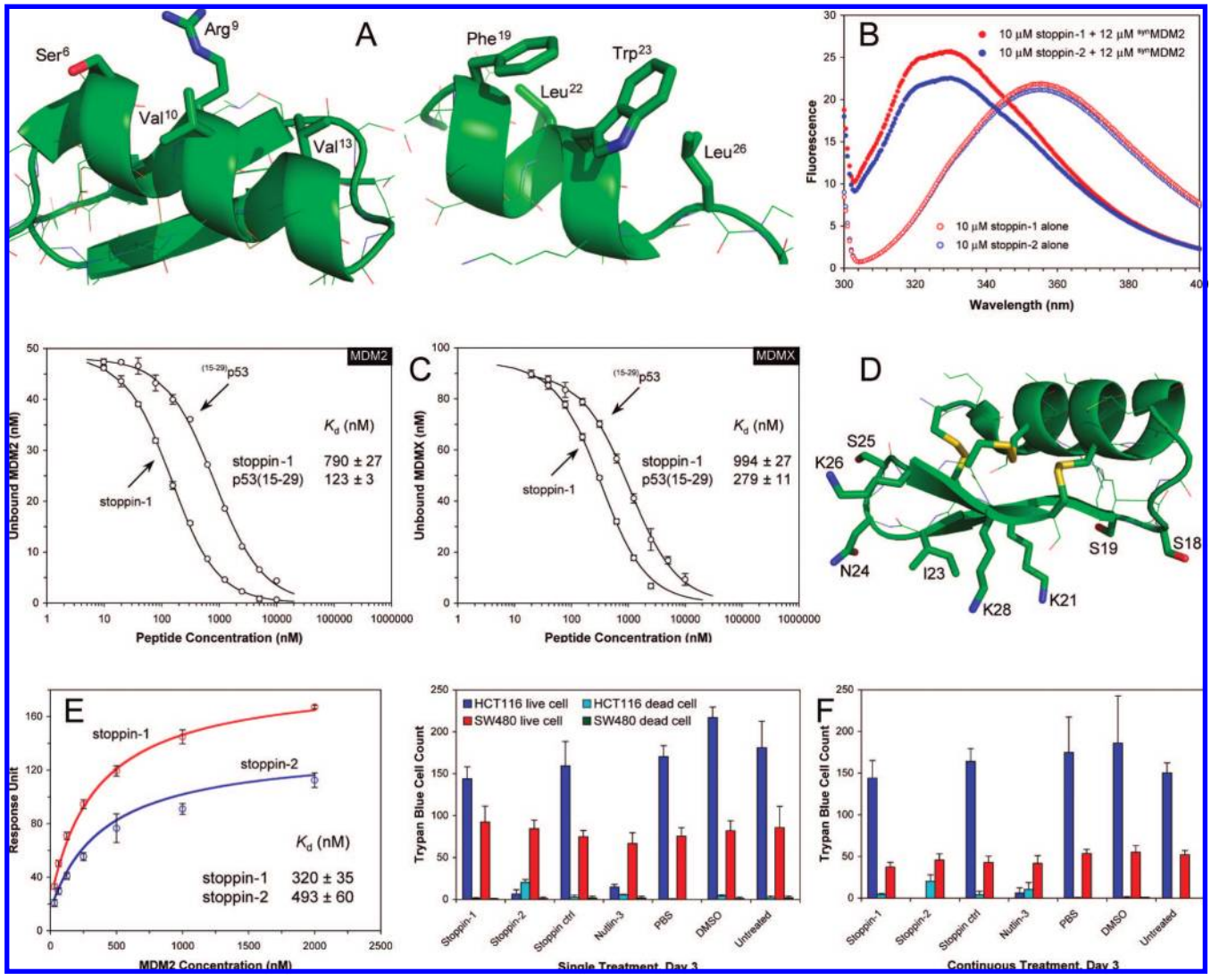

Figure 1. (A) Structural comparison between the N-terminal α-helix of BmBKTx1 and the helical segment of $^{(15-29)}$p53 complexed with $^{(17-125)}$MDM2 (created from PDB codes 1R1G and 1YCR by PyMOL, DeLano Scientific LLC). (B) Trp fluorescence spectra of stoppin-1 (red) and stoppin-2 (blue) in the absence (empty circle) and presence (filled circle) of synMDM2, obtained at room temperature in PBS using an excitation wavelength of 295 nm. (C) Quantification of the binding affinities of stoppin-1 and $^{(15-29)}$p53 for ^{syn}MDM2 (50 nM) and ^{syn}MDMX (100 nM) by SPR-based competition assays. Each curve is the mean of three independent measurements at 25 °C in 10 mM HEPES, 150 mM NaCl, 0.005% surfactant P20, pH 7.4. (D) The 1.7 Å crystal structure of synthetic BmBKTx1 showing residues in the C-terminal β-hairpin region (PDB code 1R1G). (E) Quantification of the binding affinities of immobilized stoppin-1 (red) and stoppin-2 (blue) for ^{syn}MDM2 by SPR-based direct binding assays. Each curve is the mean of three independent measurements at 25 °C in the buffer described above. (F) Tumor-killing activity of stoppin-1, stoppin-2, the stoppin-2 control (100 μg/mL), and Nutlin-3 (10 μg/mL) against HCT116 and SW480 cells as determined by Trypan blue cell count. The results from MTS cell viability assays are presented in Figure S3 in the Supporting Information. The data are averages of triplicate readings from one representative experiment.

(BmBKTx1 numbering) with Arg, creating a cluster of eight cationic residues (including three existing Lys residues) projecting from the C-terminal β-hairpin structure (Figure 1D). As these C-terminal residues are solvent exposed and distal to the MDM2/MDMX-binding α-helix at the N-terminus, minimal structural and functional perturbance are expected to ensue. An added benefit of the highly amenable mutations is elimination of potential toxic effects of stoppins on excitable cells, for the residues in the C-terminal region of scorpion toxins are involved in interactions with the K^+ channels.[4]

We synthesized and oxidatively folded stoppin-2 as well as a negative control of stoppin-2 where the Arg decoration is retained, but the MDM2/MDMX-interacting residues PheLeuTrpLeu are reverted to the native sequence SerArgValVal (Supporting Information). The native disulfide connectivity in stoppin-2 and its control, i.e., Cys^1-Cys^4, Cys^2-Cys^5, and Cys^3-Cys^6, was verified by disulfide mapping aided by chymotrypsin/trypsin digestion coupled with LC-MS analysis. Due to a strong nonspecific binding of the heavily cationic stoppin-2 to the CM5 sensor chip, however, we were unable to quantify its binding affinity for ^{syn}MDM2 and ^{syn}MDMX using the SPR-based competition assay protocol. Instead, we immobilized stoppin-1, stoppin-2, and the stoppin-2 control on CM5 sensor chips and directly quantified their interactions with ^{syn}MDM2. Steady-state binding kinetics analyses yielded K_d values of 320 and 493 nM for stoppin-1 and stoppin-2, respectively (Figure 1E). By contrast, the stoppin-2 negative control exhibited no binding, as expected, to ^{syn}MDM2. These results are entirely consistent with the data obtained from fluorescence spectroscopic studies. As shown in Figure 1B, addition of ^{syn}MDM2 to stoppin-1 or

stoppin-2 caused an identical shift of Trp fluorescence from 356 to 328 nm, suggesting that both stoppin-1 and stoppin-2 bind MDM2 in a similar fashion and likely at similar affinities.

To demonstrate the tumor-killing activity of stoppin-2, we treated cells (HCT116-$p53^{+/+}$ and the mutant p53 cell line SW480) with a single dose of stoppin-1, stoppin-2, and the stoppin-2 control at 100 μg/mL. Nutlin-3 at 10 μg/mL was used as a positive control. Expectedly, a reduction in HCT116 cell viability as measured by MTS was observed with Nutlin-3 and stoppin-2 but not with stoppin-1 and the stoppin-2 control, while none of the four compounds affected SW480 cell viability (Figure S3, Supporting Information). These effects were quantified by Trypan blue cell count. As shown in Figure 1F, left, after 3 days of single treatment, the number of HCT116 cells decreased over 90% with Nutlin-3 or stoppin-2. By contrast, the effect of stoppin-1 and the stoppin-2 control on HCT116 was minimal, and none showed measurable cell killing activity against SW480. When added daily, stoppin-2 killed HCT116 cells quantitatively (Figure 1F, right). Single treatment was less effective than continuous treatment presumably due to stoppin susceptibility to proteolytic degradation (Figure S4, Supporting Information). As was the case in the single-dose treatment, stoppin-1, stoppin-2, the stoppin-2 control, and Nutlin-3 were ineffective against SW480, so were stoppin-1 and the stoppin-2 control against HCT116. The *in vitro* data suggest that like Nutlin-3,[2c] stoppin-2 kills tumor cells in a p53-depedent manner. Further, stoppin activity appears functionally coupled with its ability to traverse the cell membrane.

The simplistic α/β fold and permissive sequence variability make sort-chain scorpion toxins ideal templates for structure-based rational design of new functionalities.[8] Even more attractive are miniprotein scaffolds with built-in cationic sequences that promote cellular uptake.[9] For p53 peptides, transition from an unbound, disordered structure to the bound, α-helical conformation costs entropy. Understandably, a miniprotein scaffold, if engineered properly to present the p53 sequence in a preformed α-helix, should in principle significantly improve binding affinity for MDM2 and MDMX. Schepartz and co-workers grafted the critical MDM2/MDMX contact residues from p53 onto the α-helical segment of the 37-residue avian pancreatic polypeptide (aPP), resulting in several miniprotein inhibitors of the p53-MDM2 interaction with low micromolar IC_{50} values.[3b] Interestingly, the inhibitory activities of aPP-derived miniprotein inhibitors correlated with the stability of the protein fold.[3b] Chen and colleagues recently demonstrated that expression via an adenovirus of thioredoxin displaying the sequence of a phage-optimized peptide inhibitor of MDM2 and MDMX resulted in efficient p53 activation, cell cycle arrest, and apoptosis of $p53^{+/+}$ tumor cells.[3a]

Stoppin-1 and stoppin-2 bind to ^{syn}MDM2 and ^{syn}MDMX several fold weaker than does the 15-residue wild type $^{(15-29)}$p53 peptide. The reason is twofold. First, the MDM2/MDMX-binding sequence of stoppins is not fully optimized. Second, the N-terminal α-helix of BmBKTx1 is not structurally identical to the helical segment of $^{(15-29)}$p53 seen in the complex with $^{(17-125)}$MDM2 (Figure 1A). In particular, Leu^{26} in p53 and Val^{13} in BmBKTx1 are not topologically equivalent because of an extra half-turn α-helix in the toxin molecule. It is plausible that introduction of helix-breaking or -destabilizing residues such as Pro and Gly to partially unwind the C-terminal portion of the α-helix of BmBKTx1 may create a side chain topology in stoppins more closely mimicking that of the p53 peptide, thus resulting in stronger antagonists of MDM2 and MDMX. In this regard, a delicate balance needs to be struck between having structural rigidity to reduce entropy loss and possessing backbone flexibility to achieve snug binding.

Acknowledgment. This work was supported in part by a Research Scholar Grant (CDD112858) from the American Cancer Society (to W.L.) and China Scholarship Council and National Basic Research Program of China (No.2007CB935800) (to C.L.).

Supporting Information Available: Synthesis and characterization of stoppin-1 and stoppin-2 by CD, fluorescence and surface plasmon resonance spectroscopy, antitumor activity assays, etc. This material is available free of charge via the Internet at http://pubs.acs.org.

References

(1) (a) Vousden, K. H.; Lane, D. P. *Nat. Rev. Mol. Cell Biol.* **2007**, *8*, 275–283. (b) Marine, J. C.; Dyer, M. A.; Jochemsen, A. G. *J. Cell Sci.* **2007**, *120*, 371–378. (c) Toledo, F.; Wahl, G. M. *Nat. Rev. Cancer* **2006**, *6*, 909–923.

(2) (a) Murray, J. K.; Gellman, S. H. *Biopolymers* **2007**, *88*, 657–686. (b) Shangary, S.; Qin, D.; McEachern, D.; Liu, M.; Miller, R. S.; Qiu, S.; Nikolovska-Coleska, Z.; Ding, K.; Wang, G.; Chen, J.; Bernard, D.; Zhang, J.; Lu, Y.; Gu, Q.; Shah, R. B.; Pienta, K. J.; Ling, X.; Kang, S.; Guo, M.; Sun, Y.; Yang, D.; Wang, S. *Proc. Natl. Acad. Sci. U.S.A.* **2008**, *105*, 3933–3938. (c) Vassilev, L. T.; Vu, B. T.; Graves, B.; Carvajal, D.; Podlaski, F.; Filipovic, Z.; Kong, N.; Kammlott, U.; Lukacs, C.; Klein, C.; Fotouhi, N.; Liu, E. A. *Science* **2004**, *303*, 844–848.

(3) (a) Hu, B.; Gilkes, D. M.; Chen, J. *Cancer Res.* **2007**, *67*, 8810–8817. (b) Kritzer, J. A.; Zutshi, R.; Cheah, M.; Ran, F. A.; Webman, R.; Wongjirad, T. M.; Schepartz, A. *ChemBioChem* **2006**, *7*, 29–31. (c) Bottger, A.; Bottger, V.; Sparks, A.; Liu, W. L.; Howard, S. F.; Lane, D. P. *Curr. Biol.* **1997**, *7*, 860–869.

(4) Xu, C. Q.; Brone, B.; Wicher, D.; Bozkurt, O.; Lu, W. Y.; Huys, I.; Han, Y. H.; Tytgat, J.; Van Kerkhove, E.; Chi, C. W. *J. Biol. Chem.* **2004**, *279*, 34562–34569.

(5) Kussie, P. H.; Gorina, S.; Marechal, V.; Elenbaas, B.; Moreau, J.; Levine, A. J.; Pavletich, N. P. *Science* **1996**, *274*, 948–953.

(6) (a) Cai, Z.; Xu, C.; Xu, Y.; Lu, W.; Chi, C. W.; Shi, Y.; Wu, J. *Biochemistry* **2004**, *43*, 3764–3771. (b) Szyk, A.; Lu, W.; Xu, C.; Lubkowski, J. *J. Struct. Biol.* **2004**, *145*, 289–294.

(7) (a) Fittipaldi, A.; Giacca, M. *Adv. Drug Delivery Rev.* **2005**, *57*, 597–608. (b) Wadia, J. S.; Dowdy, S. F. *Adv. Drug Delivery Rev.* **2005**, *57*, 579–596. (c) Brooks, H.; Lebleu, B.; Vives, E. *Adv. Drug Delivery Rev.* **2005**, *57*, 559–577.

(8) (a) Vita, C.; Drakopoulou, E.; Vizzavona, J.; Rochette, S.; Martin, L.; Menez, A.; Roumestand, C.; Yang, Y. S.; Ylisastigui, L.; Benjouad, A.; Gluckman, J. C. *Proc. Natl. Acad. Sci. U.S.A.* **1999**, *96*, 13091–13096. (b) Martin, L.; Stricher, F.; Misse, D.; Sironi, F.; Pugniere, M.; Barthe, P.; Prado-Gotor, R.; Freulon, I.; Magne, X.; Roumestand, C.; Menez, A.; Lusso, P.; Veas, F.; Vita, C. *Nat. Biotechnol.* **2003**, *21*, 71–76.

(9) (a) Smith, B. A.; Daniels, D. S.; Coplin, A. E.; Jordan, G. E.; McGregor, L. M.; Schepartz, A. *J. Am. Chem. Soc.* **2008**, *130*, 2948–2949. (b) Daniels, D. S.; Schepartz, A. *J. Am. Chem. Soc.* **2007**, *129*, 14578–14579.

JA8042036